Journal of the Korean Society of Marine Environment & Safety
Research Paper
Vol. 27, No. 6, pp. 883-889, October 31, 2021, ISSN 1229-3431(Print) / ISSN 2287-3341(Online) https://doi.org/10.7837/kosomes.2021.27.6.883

A Study on the Feasibility of Installing Solar Auxiliary Power for Small Fishing Boats

Kyoungkuk Yoon* · Hyeonmin Jeon** · Junyoung Hwang*** · Jongsu Kim**†
*, **Professor, Division of Marine System Engineering, Korea Maritime & Ocean University, Busan 49112, Korea
*** PhD Candidate, Department of Marine System Engineering, Korea Maritime & Ocean University, Busan 49112, Korea

태양광 보조전원을 설치한 소형선박의 타당성 연구

윤경국* · 전현민** · 황준영*** · 김종수**†
*, ** 한국해양대학교 기관시스템공학부 교수, *** 한국해양대학교 기관시스템공학과 박사과정

Abstract : *The South Korean fishing industry is experiencing a rapid growth owing to an increase in its leisure-fishing population. Consequently, fishing boats weighing 9-10 [ton] have also been increasing. Current fishing boats operate their essential equipment by switching their engines with batteries to reduce the cost of gas and engine noise. However, stranding incidents have been increasingly recorded annually, in which boats fail to start owing to discharged batteries, and these incidents can lead to serious casualties. This study proposes the installation of a solar auxiliary power system to safeguard fishing boats, particularly those weighing between 9-10 [ton]. The feasibility of securing space for the solar auxiliary power of boats under consideration was verified. To examine the application of solar power, this study calculates the load necessary to operate it for fishing and models such a system using an electricity analysis program The modeled system, which applies the monthly horizontal solar insolation, validated the adoption of a solar auxiliary power in fishing boats.*

Key Words : *Fishing boats, Maritime safety, Solar auxiliary power, Horizontal solar insolation, Batteries*

요 약 : 대한민국의 낚시산업은 레저활동을 즐기는 인구 증가로 인해 매년 급성장하고 있으며 이에따라 규모가 큰 9-10톤급 낚시어선의 수는 매년 늘어나고 있다. 현재 운항 중인 낚시어선은 낚시 활동 중 유류비 절감과 엔진 발생 소음 저감을 위해 엔진을 정지하고 배터리를 이용하여 선박의 필수장비를 운영하고 있다. 하지만 배터리의 방전으로 인한 엔진 시동불량 등으로 인해 해상에서 표류되는 사고가 매년 꾸준히 발생하고 있으며, 이는 대형 인명사고로 이어질 수 있다. 본 연구에서는 낚시어선의 안전확보를 위해 태양광 보조전원 설치를 제안하고, 9-10톤급 선박을 대상으로 선정하였다. 대상선박의 태양광 발전설비 공간 확보 가능성을 확인하였으며, 태양광 발전설비의 적용을 검증하기 위해 조업 중 필요한 필수 부하량을 계산하고 전력분석프로그램을 통해 태양광 발전시스템을 모델링하였다. 모델링 된 태양광 발전시스템에 우리나라의 월별 수평면 평균 일사량을 적용하여 낚시어선의 태양광 보조발전장치 적용에 관한 타당성을 입증하였다.

핵심용어 : 낚시어선, 해상안전, 태양광 보조발전시스템, 수평면 평균 일사량, 배터리

1. Introduction

Owing to an increasing income-level and leisure-fishing population, South Korea's fishing industry has been experiencing a remarkable growth. According to "The Second Master Plan to Promote Fishing" published by the Korean Ministry of Ministriy of Oceans and Fisheries, the number of people who fish leisurely for more than or equal to three times a year has increased from 5 million in 2000 to 8.5 million in 2018 (MOF, 2020a). Although the number of registered fishing boats has been relatively constant, the number of passengers and of fishing boats weighing between 9-10 [ton] have increased drastically.

Together with these trends, more than 200 fishing boat accidents have occurred annually over the past five years, as precented in

* First Author : kkyoon@kmou.ac.kr, 051-410-4265
† Corresponding Author : jongskim@kmou.ac.kr, 051-410-4831

Table 1. In 2020 alone, the number of these accidents reached 300. Their biggest cause is attributed to engine failure or propeller damage, which can lead to serious casualties. In addition, these marine accidents on fishing boats, together with the increase in the number of users of such fishing boats, could lead to significant danger on the sea (KOSIS, 2020).

Table 1. Fishing boat accidents according to their causes and years

Category	Engine Failure	Collision	Stranded (owing to coral reefs, etc.)	Floating matter	Others	Total
2016	93	26	13	21	16	169
2017	131	36	19	35	14	235
2018	120	36	18	22	36	232
2019	135	43	21	43	36	278
2020	151	51	26	38	35	301
Subtotal	630	192	97	159	137	1,215

Current fishing boats operate their essential equipment by switching their engine functions with batteries to reduce the cost of gas and engine noise. However, a protracted use of a battery in lieu of the engine can trigger its discharge, which can lead to a serious stranding accident and casualties on the sea.

This study proposes the installation of a solar auxiliary power system to help reduce fishing boat accidents among boats weighing 9 ‐ 10 [ton]. To validate the advantage of a solar auxiliary power for such fishing boats, possible placements of the solar auxiliary power generating unit were determined. The appropriate capacity of the power generating unit and battery, including the charge and discharge devices, according to their varying possible placements, were also determined. The feasibility of the installation of a solar auxiliary power system on fishing boats was validated via power analysis simulations.

2. Investigation of fishing boats with solar auxiliary power

As presented in Table 2, the total number of registered fishing boats in South Korea was 4536 in 2020. Among these, boats weighing between 9-10 [ton] were the most common at 1082, those weighing between 3-4 [ton] were at 868, and those weighing between 4-5 [ton] were at 661. Compared to 2016, the number of fishing boats weighing 9 ‐ 10 [ton] have experienced the most significant increase by 403, owing to the drastic increase in the number of leisure-fishing passengers. Therefore, this study considers boats weighing 9 ‐ 10 [ton], which are the most registered types of coastal fishing vessels (MOF, 2020b).

Table 2. Registered boats according to their weight

	0~1	1~2	2~3	3~4	4~5	5~6	6~7	7~8	8~9	9~10	total
‘16	59	656	738	776	701	144	302	380	65	679	4500
‘17	45	560	690	840	676	137	299	423	58	759	4487
‘18	31	487	647	881	680	130	317	454	60	856	4543
‘19	28	447	625	806	659	133	300	449	72	976	4595
‘20	25	407	545	868	661	127	291	446	84	1082	4536
	▼34	▼249	▼193	▲92	▼40	▼17	▼11	▲66	▲19	▲403	

Fig. 1 presents a schematic diagram of a fishing boat weighing 9 ‐ 10 [ton]. The legally required equipment on such a coastal fishing vessel includes V-PASS, VHF, SSB radio, fishfinder, floater, and radar; in addition, the required power for evacuation (including lighting system) is approximately below 1 [kW] (KMI, 2011).

The specifications of the fishing vessel in consideration were 9.16 [ton] in weight, 16.24 [m] long, and 4.37 [m] wide. A crane was installed at the bow side, which did not allow the solar auxiliary power system to be installed there. Therefore, the solar auxiliary power generation system was positioned above the wheelhouse on the stern side. Various antennae and GPS receivers were installed in the upper part of the wheelhouse for the vessel’s navigation. The space available for installing commercialized solar panels was approximately 3 [m] long and 2 [m] wide, which could enable a maximum power generation of 1 [kW].

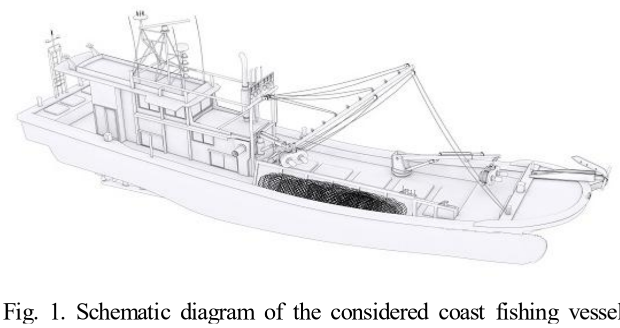

Fig. 1. Schematic diagram of the considered coast fishing vessel.

3. Design of the solar auxiliary power generation system

3.1 Principle of the solar auxiliary power generation system

Fig. 2 presents a diagram that elucidates the principle of solar power generation. Solar power generation is a technology that converts solar energy into electricity, owing to the photoelectric effect of solar cells.

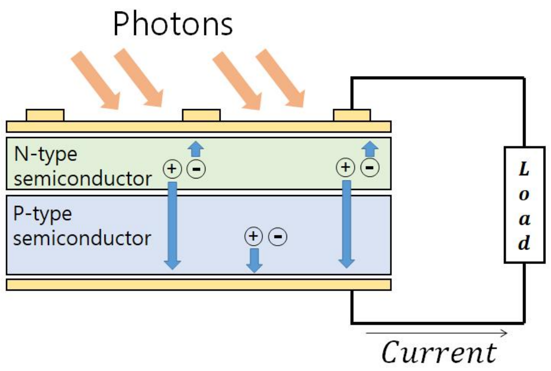

Fig. 2. Principle of solar power generation.

Assuming the attribute of light as a particle, photoelectric effect occurs when light is irradiated onto a metal, and current flows as triggered by the energy of photons. The energy of a photon B is expressed in Equation (2-1).

$$B = hf = hc/\lambda \tag{2-1}$$

Here, h, f, c, and λ denote the Planck constant, frequency, speed of light, and wavelength of the light, respectively.

3.2 Power converter

A solar power generation system harnesses a boost converter to boost the voltage. Fig. 3 illustrates the circuit of the boost converter (Won et al., 2015). The operation of the boost converter can be divided into ON and OFF. When the switch is ON, the current on the inductor side increases in proportion to the size of the inductance "L." The energy charged in the capacitor is in a reverse-biased diode and is cut off, and the stored energy is supplied to the load side. Conversely, to increase the output voltage, when the switch is OFF, the energy stored in the inductor and the input power are introduced and transferred to the load side while charging the capacitor.

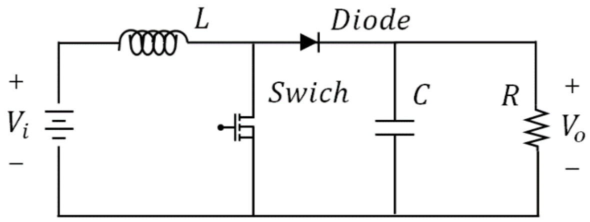

Fig. 3. Configuration of power conversion device for the solar power generation system.

3.3 MPPT Controller

Fig. 4 presents a voltage-current characteristic curve of a solar cell (Enslin et al., 1997). The X- and Y-axes represent the terminal voltage V_{sa} axis of the solar cell and its current output I_{sc}, respectively. When the load resistance is 0 [Ω], the terminal voltage is also 0 [V], and the current is the short-circuit current I_{sc}. When the load resistance is increased, the terminal voltage also increases, while the terminal current decreases. When the load resistance is ∞ [Ω], the terminal voltage V_{sa} becomes an open-circuit voltage V_{oc}, and the terminal current I_{sa} becomes 0 [A].

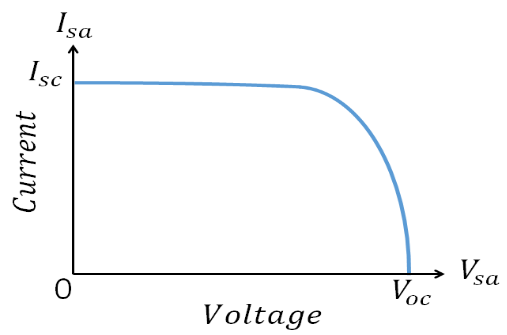

Fig. 4. Voltage-current characteristic curve of a solar cell.

Using the solar cell voltage-current characteristic curve in Fig. 4, the power-voltage characteristic curve can be drawn as illustrated in Fig. 5. The X- and Y-axes represent the solar cell terminal voltage V_{sa} and the output power P_{sa}, respectively. On this power-voltage characteristic curve, there is a point at which the output power of the solar cell is maximum (Hussein et al., 1995). This point is called the maximum power point (MPP), and the voltage at this point is called the maximum power voltage V_{mpp}. Because the maximum power point and maximum power voltage vary with the amount of light incident upon the solar cell and its temperature, to increase the controller efficiency, controlling the MPP is critical.

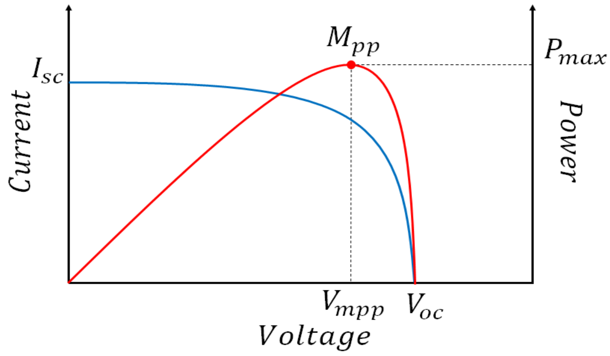

Fig. 5. Power-voltage characteristic curve.

Among the several control methods used to track the MPP and increase the efficiency of the solar power generation system controller, the perturb and observe (P&O) control method is the most widely used method, owing to its simple feedback structure and small number of parameters (Femia et al., 2020). Fig. 6 presents a flowchart of the algorithm for the P&O control method.

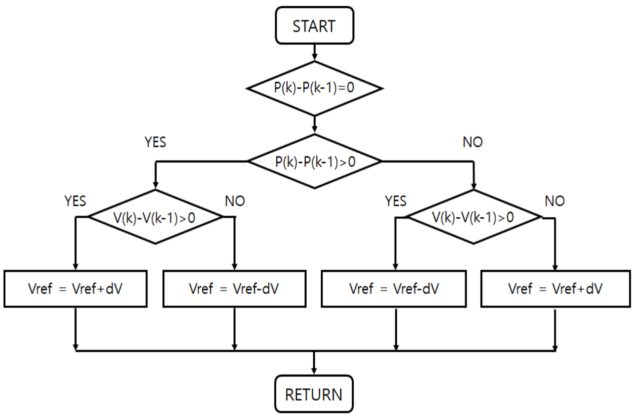

Fig. 6. P&O control method of solar power regeneration.

The P&O control method compares the current output power of the solar cell's module with the output power during its previous cycle, then adjusts the reference voltage at regular intervals to continuously locate the maximum operating point. The voltage $V(k)$ and current $I(k)$ are measured at the output side of the solar cell and multiplied together to calculate the power $P(k)$. The change in the reference voltage is determined by the change in the power and voltage of the previous cycle (represented as $P(k-1)$ and $V(k-1)$, respectively). If the current power $P(k)$ is greater than the previous power $P(k-1)$, and the reference voltage was increased in the previous cycle, the voltage is subsequently increased in the current cycle. Likewise, if the voltage was decreased, it is decreased in the current cycle. Conversely, if the current power $P(k)$ is smaller than the previous power $P(k-1)$, and the reference voltage was increased in the previous cycle, the voltage is decreased in the current cycle. If the reference voltage was decreased in the previous cycle, it is increased in the current cycle.

4. Modeling of the solar power generation system for the vessel under consideration

4.1 Solar power generation system

Fig. 7 presents a simulation of a solar power generation system for a 9.16 [Ton] fishing boat with 1 [kW] power generation capacity. In addition, 160 [W] capacity panels were configured in series and parallel to a capacity of approximately 1 [kW], and comprised a lithium-ion battery for storing the electricity generated from sunlight and a DC-DC converter (a power converter).

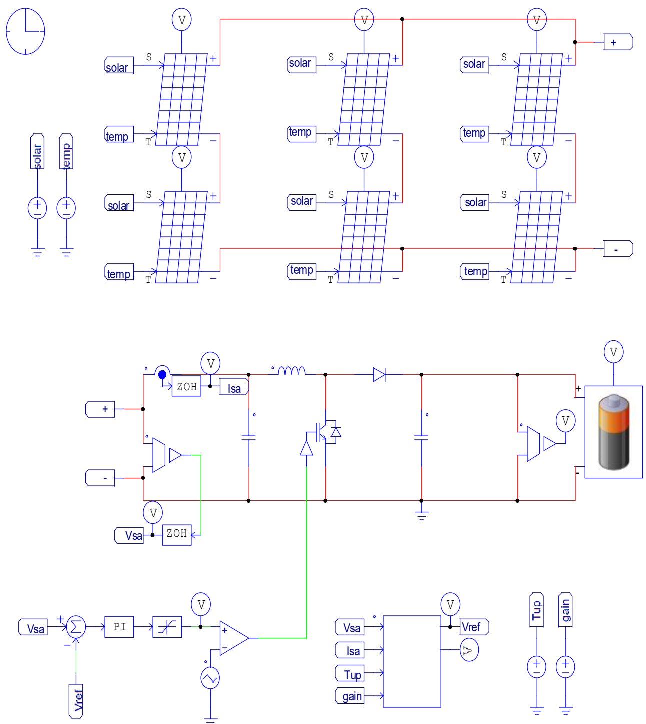

Fig. 7. Complete configuration of the solar power generation system.

Fig. 8 illustrates the P&O control method's maximum power point tracking (MPPT) controller implemented in a C-box to optimally store the power in the battery.

```
#include <Stdlib.h>
#include <String.h>
#include <math.h>
#include <Psim.h>

{
double Vsa, Isa, DV;
int TUpdate;
double Psa, flag;
static int i=0;
static double Psa_old=10.0, Vsa_old=0.0, Vref=0.0;

Vsa = in[0];
Isa = in[1];
DV = in[2];
TUpdate = in[3];

i++;
if((i%TUpdate==0)){
        Psa = Vsa*Isa;
        if(Psa>=Psa_old){
                if(Vsa>Vsa_old)Vref=Vref+DV;
                else Vref=Vref-DV;
        }
        else{
                if(Vsa>Vsa_old)Vref=Vref-DV;
                else Vref=Vref+DV;
        }
        Psa_old=Psa;
        Vsa_old=Vsa;
}
out[0] = Vref;
out[1] = i;
}
```

Fig. 8. Implementation of MPPT controller of a solar power generation system.

4.2 Battery system

Fig. 9 presents the parameters of the battery adopted in the solar power generation system. Considering the space of the fishing boat, “VL-34570” model lithium-ion batteries of 3.7 [V] and 5.4 [Ah] were utilized. To obtain the required battery capacity, 189 batteries in series and 15 in parallel were connected to form a battery module with voltages at 700 [V], 81 [Ah].

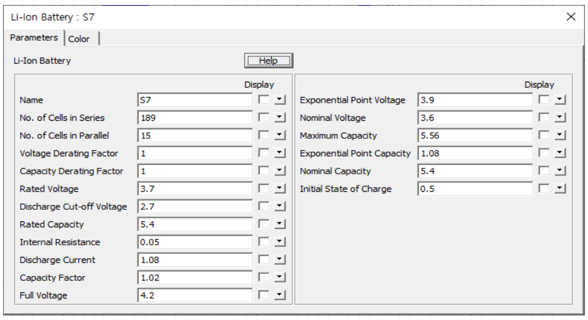

Fig. 9. Module battery configuration.

4.3 Boost converter

To store the output of the solar power generation system in the battery, it is necessary to boost the output voltage. A boost converter comprising an IGBT (a typical semiconductor switching device), a diode, an inductor, and a capacitor, was designed to achieve this objective.

5. Simulation result analysis

Table 3 presents the data of South Korea's monthly horizontal solar insolation and monthly available power generation time converted appropriately into the simulation environment, which are provided by the Korea Institute of Energy Research. The average insolation per hour [kWh/㎡/day] was calculated by dividing the average insolation [kWh/㎡/day] on the given horizontal surface by the average daily power generation time (Korea Institute of Energy Reserch, 2020). The unit of insolation was converted to [W/㎡].

Table 3. Monthly horizontal solar insolation and monthly available power generation time

	JAN	FEB	MAR	APR	MAY	JUN	JUL	AUG	SEP	OCT	NOV	DEC
Monthly insolation	2211	2820	3303	3980	4307	3963	3623	3804	3120	2965	2324	2055
Generation time	2.45	3.43	4.58	5.28	4.46	4.37	3.04	3.42	3.53	3.89	2.93	2.64
Hourly insolation	902	822	721	754	966	907	1192	1112	884	762	793	778
Insolation	1049	956	838	876	1122	1054	1385	1293	1027	886	922	905

Fig. 10 shows the simulation results obtained when the average monthly solar radiation [W/㎡] was applied (SolarConnect, 2020). Table 4 presents the average monthly output and monthly average solar power generation. December had the lowest monthly average solar radiation at 2055 [kWh/㎡/day], while May had the highest at 4307 [kWh/㎡/day]. Considering the daily average power generation time and converting to hourly insolation, the average output was the lowest in March at 721 [kWh/㎡/day], and the highest in July at 1192 [kWh/㎡/day]. Simulation results obtained with the considered fishing vessel yielded average outputs of 0.91 [kW] in March (lowest) and 1.49 [kW] in July (highest).

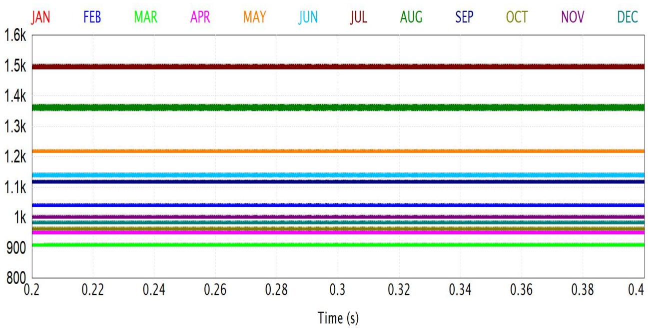

Fig. 10. Simulation results using monthly insolation.

Table 4. Monthly average output and power generation of the solar power generation system

	JAN	FEB	MAR	APR	MAY	JUN	JUL	AUG	SEP	OCT	NOV	DEC
Average output (kW)	1.14	1.04	0.91	0.95	1.21	1.14	1.49	1.36	1.11	0.96	1.00	0.98
Generated power (kW/d)	2.79	3.57	4.17	5.02	5.43	4.99	4.55	4.66	3.95	3.75	2.93	2.60

To verify the status of the solar power generation system, Figs. 11 and 12 present the reference voltage, output voltage, and current of the solar controller under the solar cell's standard test condition (insolation at 1000 [W/㎡]). As illustrated on the graph, the reference voltage and solar output voltage are unstable in the initial transient state. However, it graph exhibits the maximum power voltage at 0.03 [sec], and the solar output voltage is stable at 34.4 [V] at 0.07 [sec]. In the current graph, the solar output current is stabilized at 31.5 [A] at 0.07 [sec].

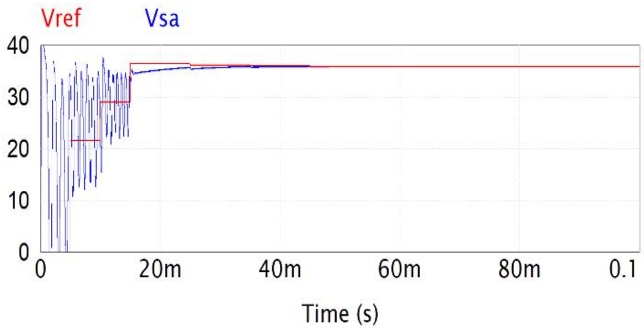

Fig. 11. Output voltage of solar controller at standard insolation.

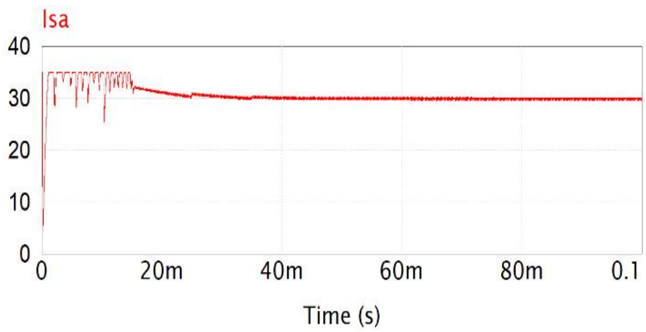

Fig. 12. Output current of solar controller at standard insolation.

Fig. 13 indicates that the state of charge (SOC) of the battery increased as expected because the battery was charged under the standard test condition of insolation (1000 [W/㎡]).

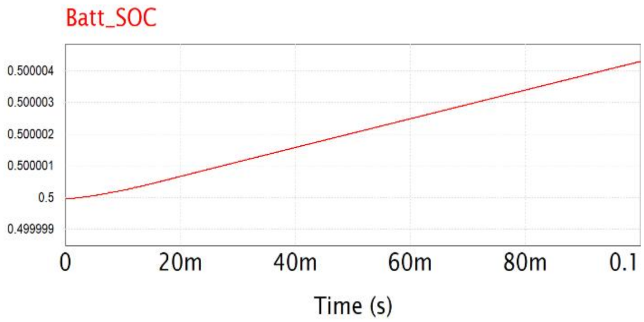

Fig. 13. Condition of battery under standard test condition.

6. Conclusion

This study proposed the installation of a solar auxiliary power generation system to ensure the safety of fishing boats. To validate the feasibility of installing the solar power generation system, this study considered fishing boats weighing between 9-10 [Ton], which are also the most registered types of boats. The required load for the operation of the considered vessel was calculated to identify an appropriate space to install the solar power generation system. Furthermore, the solar power generation system was modeled with a power analysis program to verify the advantage of the solar power generation equipment. When the monthly horizontal insolation of the Korean coastal waters was applied, the average output was 0.91 [kW] in March (lowest), and 1.49 [kW] in July (highest). Hence, the feasibility of the installation and application of the solar auxiliary power generation system was verified as an effective means of reducing safety accidents among fishing boats.

Acknowledgements

This research was supported by the Korea Institute of Marine Science & Technology Promotion (KIMST) grant funded by the Ministry of Oceans and Fisheries in 2021. (NO 20210369)

References

[1] Enslin, J. H. R., M. S. Wolf, D. B. Snyman, and W. Swiegers(1997), Integrated photovoltaic maximum power point tracking converter, IEEE, Vol. 44, Issue 6, pp. 769-773.

[2] Femia, N., G. Petrone, G. Spagnulol, and M. Vitelli(2005), Optimization of perturb and observe maximum power point tracking method, IEEE, Vol. 20, Issue 4, pp. 963-973.

[3] Hussein, K. H., I. Muta, T. Hoshino, and M. Osakada(1995),

Maximum photovoltaic power tracking: An algorithm for rapidly changing atmospheric conditions, In Proc. Inst. Elect. Eng., Vol. 142, No. 1, pp. 59-64.

[4] KMI(2011), Korea Maritime Institute, Measures for Added-value Creation of the Korean Recreational Fishing Industry, Busan, Korea.

[5] Korea Institute of Energy Reserch(2020), Analysis of Solar Insolation in 2020, Daejeon, Korea

[6] KOSIS(2020), Korean Statistical Information Service, Status of Marine Accidents by Ship Use, Daejeon, Korea.

[7] MOF(2020a), Ministry of Oceans and Fisheries, Second Master Plan to Promote Fishing, Sejong, Korea.

[8] MOF(2020b), Ministry of Oceans and Fisheries, Current status of fishing boats, Sejong, Korea.

[9] SolarConnect(2020), Inc., Analysis of Photovoltaic Time in 2020, Seoul.

[10] Won, C. Y., Y. R. Kim, T. K. Lee, Y. C. Jeong, and B. K. Lee(2015), Electrical and electronics, Hanbit Academy.

Received : 2021. 08. 25.
Revised : 2021. 09. 16.
Accepted : 2021. 10. 28.